

Integration of Blood Outgrowth Endothelial Cells in Dermal Fibroblast Sheets Promotes Full Thickness Wound Healing

BENOIT HENDRICKX,^{a,b} KRISTOFF VERDONCK,^{a,b} STEFAAN VAN DEN BERGE,^b STIJN DICKENS,^b ELOF ERIKSSON,^c JAN JEROEN VRANCKX,^b AERNOU LUTTUN^a

^aCenter for Molecular and Vascular Biology, ^bDepartment of Plastic, Reconstructive and Aesthetic Surgery, KULeuven, Leuven, Belgium; ^cLaboratory of Tissue Repair and Gene Transfer, Harvard Medical School, Division of Plastic Surgery, Brigham and Woman's Hospital, Boston, USA

Key Words. Endothelial cells • Angiogenesis • Autologous stem cell transplantation • Hypoxia • Peripheral blood stem cells • Progenitor cells • Tissue regeneration • Skin grafts

ABSTRACT

Vascularization is the cornerstone of wound healing. We introduced human blood outgrowth endothelial cells (hBOEC) in a self-assembled human dermal fibroblast sheet (hDFS), intended as a tissue-engineered dermal substitute with inherent vascular potential. hBOEC were functionally and molecularly different from early endothelial progenitor cells and human umbilical vein endothelial cells (HUVEC). hBOEC alone, unlike HUVEC, efficiently revascularized and re-oxygenated the wound bed, both by active incorporation into new vessels and by trophic stimulation of host angiogenesis in a dose-dependent manner. Furthermore, hBOEC alone, but not HUVEC, accelerated epithelial coverage and matrix organization of the wound bed. In addition,

integration of hBOEC in hDFS not only further improved vascularization, epithelial coverage and matrix organization but also prevented excessive wound contraction. In vitro analyses with hBOEC, fibroblasts and keratinocytes revealed that these effects were both due to growth factor crosstalk and to short cutting hypoxia. Among multiple growth factors secreted by hBOEC, placental growth factor mediated at least in part the beneficial effects on keratinocyte migration and proliferation. Overall, this combined tissue engineering approach paves the way for clinical development of a fully autologous vascularized dermal substitute for patients with large skin defects that do not heal properly. *STEM CELLS* 2010;28:1165–1177

Disclosure of potential conflicts of interest is found at the end of this article.

INTRODUCTION

Wound healing restores the barrier function of skin by hemostasis, matrix deposition/remodeling, re-epithelialization, vascularization, and contraction. These processes are not separately/sequentially activated, but closely interact through multidirectional crosstalk between cellular players: platelets, inflammatory cells, (myo)fibroblasts, keratinocytes, endothelial cells (EC), and smooth muscle cells (SMC) [1, 2]. Not only do these cells secrete factors for fine-tuning the healing process, they also produce and modulate the extracellular matrix (ECM) using proteolytic tools [e.g., matrix metalloproteases (MMP)] [2, 3]. The ECM is the dermis' structural component and acts as a guidance grid for cell migration [1, 3]. In the later phases of wound healing, the initially deposited jumbled ECM is remodeled by proteases, allowing fibroblasts to produce a highly organized dermal fiber network. Although hypoxia triggers processes that initiate the response to injury, those later phases of wound healing strongly depend on

appropriate oxygen delivery [4, 5]. As deficient oxygen supply is the major cause of impaired wound repair, vascularization, as the delivery route for oxygen, really is the cornerstone of wound healing [6–8].

Postnatal vessel formation encompasses two processes: angiogenesis (EC sprouting from pre-existing tubes) and vasculogenesis (tubular coalescence of blood-borne EC progenitors) [9]. Endothelial progenitor cells (EPC) were first described in 1997 (ref. [10]). Since then debate has arisen concerning their identity, derivation, and function [11, 12]. Later, Yoder et al. redefined EPC taking into account their outgrowth and adhesion kinetics and their direct contribution to vessel growth by vascular incorporation [11]. According to this definition, two EPC types are distinguished: the early outgrowing and initially nonadherent fraction, which is clonally related to hematopoietic stem cells and does not incorporate into vessels, and the late outgrowing and immediately adherent fraction that lacks hematopoietic markers and does incorporate into vessels [11]. The latter cells are also referred to as “blood outgrowth endothelial cells” (BOEC) and have been

Author contributions: B.H.: conception and design, collection and assembly of data, data analysis and interpretation, manuscript writing; K.V. and S.VdB.: conception and design, provision of study material, manuscript writing; S.D.: collection and assembly of data, data analysis and interpretation; E.E.: manuscript writing; J.J.V.: manuscript writing, final approval of the manuscript; A.L.: conception and design, data analysis and interpretation, manuscript writing, final approval of the manuscript.

Correspondence: Aernout Luttun, Ph.D., Center for Molecular and Vascular Biology, Katholieke Universiteit Leuven, Campus Gasthuisberg, Onderwijs & Navorsing 1, Herestraat 49, B-3000 Leuven, Belgium. Telephone: +3216345772; Fax: +3216345990; e-mail: aernout.luttun@med.kuleuven.be Received December 9, 2009; accepted for publication May 10, 2010; first published online in *STEM CELLS EXPRESS* May 18, 2010. © AlphaMed Press 1066-5099/2009/\$30.00/0 doi: 10.1002/stem.445

derived from peripheral and/or cord blood [13–16]. They have been used for restoring blood flow in peripheral vascular disease models [17, 18], for prevascularization of decellularized skin or bone tissue-engineered constructs [19, 20] and as a vehicle for gene therapy [15, 21]. Although the ability to infiltrate in vessels is a well-recognized feature of BOEC, their trophic effect on neovascularization is not well-documented and even doubted [12], neither have their paracrine interactions with non-EC been elaborately studied, certainly not in a wound context. Apart from EPC, other (stem) cell sources have been considered to vascularize wounds and efforts have mostly been made in the field of mesenchymal stem cells (MSC) [22, 23]. In addition to cell therapy, angiogenic growth factor therapy [e.g., vascular endothelial growth factor (VEGF), basic fibroblast growth factor (bFGF), platelet-derived growth factor (PDGF), and placental growth factor (PIGF)] has been explored to grow vessels in nonhealing or chronic wounds [24–26].

Even though cells and growth factors alone may assist in accelerating wound vascularization and healing, defects larger than four centimeter in diameter due to, for example, burns, do not properly heal without a skin graft [27]. In those wounds, split-thickness skin grafts still are “the gold standard” for skin restoration. However, these merely restore the epidermis, resulting in brittle skin prone to excessive contraction. Tissue-engineered skin equivalents have been proposed to overcome this [27]. To avoid immune rejection, the design of a fully autologous construct is paramount. Of equal importance, survival of such skin equivalents critically depends on quick and functional vascularization [27]. We explored the use of human blood outgrowth endothelial cells (hBOEC) to enhance wound vascularization and investigated the mechanisms by which this promotes the reciprocal dialogue of cellular players during healing. In addition, in an effort to develop a clinically usable autologous skin equivalent for large skin defects, we tested the potential of hBOEC to vascularize multilayered human dermal fibroblast sheets (hDFS) in full thickness wounds.

MATERIALS AND METHODS

An extended methods section is available as Supporting Information.

Cell Derivation, Culture, Characterization, and Transduction

hBOEC, Early EPC, and Human Umbilical Vein Endothelial Cells. Peripheral blood samples were obtained from healthy volunteers. Mononuclear cells were isolated by density centrifugation and hBOEC and early EPC were obtained using a slightly modified protocol by Yoder et al. [11] and Hill et al. [28], respectively. Human umbilical vein endothelial cells (HUVEC) were obtained as described in the Supporting Information. Cells for experiments were from passage (P)2–4 (hBOEC) or P4–7 (HUVEC).

Human Dermal Fibroblast Sheets. Dermal fibroblasts were isolated from skin after incubation with dispase II and collagenase type IA. Fibroblasts were expanded up to P3 and grown into multilayered lawns that were engineered into three-dimensional sheets (Fig. 1L).

hKeratinocytes. hKeratinocytes were isolated from foreskins and cultured in serum-free and growth factor-containing media. P3–5 cells were used in experiments.

Characterization. Cell cultures were analyzed under various conditions for their expression profile by quantitative reverse transcriptase-polymerase chain reaction (qRT-PCR). hBOEC, HUVEC, and early EPC were phenotyped by fluorescence-activated cell sorting (FACS) and/or immunofluorescence (antibody list: Supporting Information Table S1) and were functionally evaluated by the DiI-acetylated low-density lipoprotein (AcLDL) uptake assay, Ulex Europaeus Agglutinin (UEA)-lectin binding and by tube formation on matrigel. hDFS incubated in normoxic (20% O₂) or hypoxic (1% O₂) conditions, were characterized after fixation, embedding, and sectioning. Sirius-red (SRed)-stained sections were used for analyzing matrix deposition (bright light) and organization (polarized light).

Lentiviral Transduction. hBOEC were transduced as described in the Supporting Information. Transduction efficiency was monitored by FACS and was ~100% for all viruses (not shown). Virus constructs used were: PGK-GFP, pTripMR1-CMVDsRed-scrambled_shRNA and pTripMR1-CMVDsRed-shPIGF1 (PIGF^{KD}; Supporting Information Figure S1). Knock-down efficiency was monitored by enzyme-linked immunosorbent assay (ELISA) on supernatant. All experiments involving human donors were performed with approval of the Ethical Committee of the University Hospital, UZLeuven.

Mice, Surgery, Transplantation, Live Imaging, and Follow-up

Full thickness wounds (0.5-cm diameter) were made on the back of athymic nude Foxn1 males (Supporting Information Note S1), splinted with a silicone ring (Fig. 2A; Supporting Information Note S2) and treated with saline, 5×10^5 or 1.5×10^6 hBOEC, 5×10^5 HUVEC, hDFS or hDFS seeded with 5×10^5 hBOEC. In some animals, hBOEC were labeled with DiI-AcLDL before transplantation or transduced with phosphoglycerate kinase-green fluorescent protein (PGK-GFP). Every other day, digital pictures of the wounds were taken (using a NikonD1 camera and Camera-Control-Pro software) under isoflurane anesthesia and the dressing was renewed. Wound blood flow was monitored by scanning the area including the entire ring with a Lisca-PIM-II (Gambro, Breda, The Netherlands; Supporting Information Figure S2), using the skin region under the processus xiphoideus for normalization. Electron paramagnetic resonance oximetry was performed 24 hours after implantation of Lithium-Phtalocyanin crystals [29]. Live imaging of cell engraftment was performed under anesthesia using a Zeiss Lumar dissection microscope. Wound contraction was evaluated as described in the Supporting Information. Mouse procedures were performed according to the guidelines of the Institutional Animal Care and Use Committee of KULeuven.

Tissue Processing, Histology, and Microscopy

At day 5 or 10 after wounding, mice were sacrificed and skin fragments including the wound area and a rim of normal skin were dissected out, fixed, separated in two pieces at the midline and processed for paraffin or optimal cutting temperature (OCT) embedding. In some mice, half of the tissue was fixed for semithin sectioning and transmission electron microscopy (TEM). For all stainings and analyses, 7- or 8- μ m sections were used spanning a representative area of ~0.7–1.4 mm. Hematoxylin/eosin and SRed stainings were performed as described [30]. Detection of hypoxic cells was done using HypoxyprobeTM, according to the manufacturer’s instructions (Millipore, Brussels, Belgium) [8]. For immunohistochemistry/fluorescence, an antibody list is provided in Supporting Information Table S1. Pictures for morphometric analysis were taken using a Zeiss Axio Imager connected to an Axiocam MRc5 camera and analysis/image recording was performed using Axiovision (Zeiss,

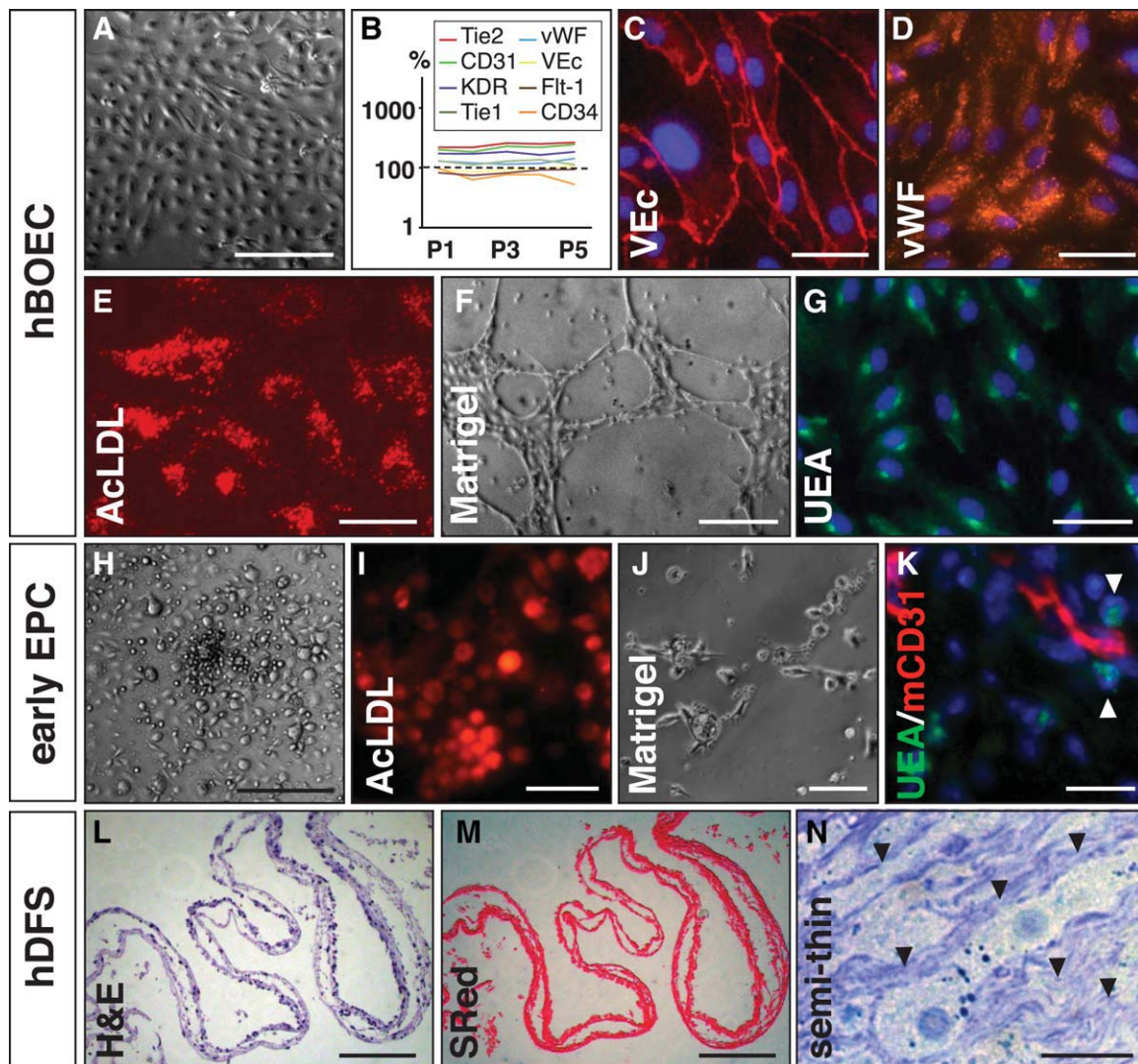


Figure 1. Characterization of hBOEC, early EPC, and hDFS. (A): Phase-contrast picture showing a cobble-stone hBOEC colony. (B): Diagram revealing stable expression of endothelial markers (*vWF*, *KDR*, *Flt-1*, *Tie-2*, *VE-cadherin*, and *CD31*) and a slight downregulation of *CD34* (in yellow) during five passages (P). Data were normalized to GAPDH and expressed as % versus HUVEC (dashed line indicates expression level in human umbilical vein endothelial cells). (C, D): hBOEC expressed VEC [red in (C)] and vWF [red in (D)] in a typical pattern. (E–G): hBOEC functionally behaved like endothelial cells, as shown by AcLDL uptake [red in (E)], tube formation on matrigel (F) and UEA-lectin binding [green in (G)]. (H): Phase-contrast picture showing an early EPC colony consisting of small round cells in the center and flattened cells around. (I–K): Although early EPC take up AcLDL [red in (I)], they did not form tubes on matrigel (J) and did not incorporate into murine host vessels [stained with CD31 in red in (K)] *in vivo* but were located along the vessels, as shown by UEA-lectin staining [green in (K)]. (L–N): hDFS revealed on cross-sections by H&E (L), SRed (M), and on toluidine-blue-stained semithin sections (N). Arrowheads in (N) indicate extracellular matrix. 4',6-diamino-2-phenylindole (DAPI) (blue) was used as nuclear counterstain in (C, D, G, K). Scale bars: 10 μ m in (N), 25 μ m in (I), 50 μ m in (J), 100 μ m in (C, D, E, G, K, L, M), 200 μ m in (F), 250 μ m in (H), and 500 μ m in (A). Abbreviations: AcLDL, acetylated low-density lipoprotein; EPC, endothelial progenitor cells; Flt-1: fms-like tyrosine kinase-1; GAPDH: glyceraldehyde 3-phosphate dehydrogenase; hBOEC, human blood outgrowth endothelial cells; hDFS, human dermal fibroblast sheets; H&E, hematoxylin and eosin; KDR, kinase insert domain receptor; SRed, Sirius-red; UEA, Ulex Europaeus Agglutinin; VEC, vascular endothelial-cadherin; vWF, von Willebrand factor.

Zaventem, Belgium), ImageJ or KS300 (Leica, Aartselaar, Belgium) software.

RNA, qRT-PCR, Cytokine Production, Cell Proliferation/Migration Assays

RNA Isolation, Quantitative (q)RT-PCR. Total RNA from cell lysates was extracted using the RNeasy minikit (Qiagen, Valencia, CA). mRNA was reverse transcribed using Superscript II Reverse Transcriptase (Invitrogen, Merelbeke, Belgium). Primers are listed in Supporting Information Table S2. mRNA levels were normalized using GAPDH or β -actin as housekeeping gene. For comparative qRT-PCR on samples in 1% or 20% O₂, hypoxan-

thine phosphoribosyltransferase-1 was used as housekeeping gene (Supporting Information Figure S3 and Note S3).

Cytokine Production. hBOEC, HUVEC, or hDFS were plated/incubated at high confluence in the appropriate media and supernatant was collected. Protein concentration was determined by the Bradford assay. ELISA kits were from R&D Systems (Abingdon, UK). Zymography and Western blot was performed as described in the Supporting Information.

Cell Proliferation/Migration. For hKeratinocyte proliferation assays, cells were plated on collagen type I-coated plates at low confluence in growth media in 1% or 20% O₂ conditions, with

addition of 10 ng/ml recombinant human (rh)PIGF (R&D Systems, Abingdon, UK) or in the presence of 90 hours conditioned media collected from hBOEC or hDFS or growth media incubated for 90 hours in the absence of cells [nonconditioned media (NCM)]. Ten days after plating, cells were harvested and counted with a NucleoCounter (ChemoMetec, Vilvoorde, Belgium). hKeratinocyte migration was evaluated in collagen type I-coated plates by measuring the area taken up by the cells in a 1-mm window, 6 or 24 hours after applying a standardized scratch wound in confluent cultures of keratinocytes grown under 1 or 20% O₂ or in the presence of (non-)conditioned media or rhPIGF.

Statistical Analysis

Comparison of data, expressed as mean \pm SEM, was performed using the unpaired Student's *t*-test. A Kolmogorov–Smirnov test was used to verify that the data had a Gaussian distribution, which justified the use of a parametric test. Differences were considered significant when $p < .05$.

RESULTS

hBOEC, HUVEC, Early EPC, and hDFS Characterization

Unlike early EPC appearing in the replated mononuclear fraction as colonies with central rounded cells and flat cells radiating from the center after 4–7 days (Fig. 1H), colonies with cobble-stone morphology (Fig. 1A) grew out later (15 days) from the collagen-adherent mononuclear fraction of peripheral blood (Supporting Information Table S3 and Note S4). qRT-PCR revealed robust EC marker expression [*von Willebrand factor* (*vWF*), *Tie-1*, *Tie-2*, *fms-like tyrosine kinase-1* (*Flt-1*), *kinase insert domain receptor* (*KDR*), *vascular endothelial-cadherin* (*VE-cadherin*), *endothelial nitric oxide synthase* (*eNOS*), *CXCR4*, *CD31*, and *CD34*], which remained stable until P5, except for *CD34* expression that decreased in later passages (Fig. 1B; Supporting Information Table S4). hBOEC, like HUVEC, uniformly expressed *vWF*, *VE-cadherin*, *KDR*, *Tie-2*, and *CD31* protein (Fig. 1C, 1D and Supporting Information Figure S4A–C,E–G), whereas early EPC expressed lower levels of these proteins (Supporting Information Figure S4I–K). Consistent with another study [31], hBOEC expressed little *AC133*, an EPC marker, but were distinguished from terminally differentiated EC by their higher expansion capacity and a distinct growth factor expression pattern (Table 1). Unlike early EPC, hBOEC did not express *CD45* (Supporting Information Figure S4H,I and Table S4), expressed lower levels of β_2 -*integrin* (*CD18*), yet higher levels of *bone morphogenetic protein-2* and *-4* and *eNOS* (Supporting Information Table S4), as described [13, 18, 32]. *MMP-9* expression was lower in hBOEC compared with early EPC (Supporting Information Table S4). hBOEC functionally behaved as EC, demonstrated by AcLDL uptake, tube formation on matrigel and UEA-lectin binding (Fig. 1E–1G). Early EPC took up AcLDL but did not efficiently form tubular structures on matrigel (Fig. 1I, 1J). Human dermal fibroblasts were tissue-engineered into a multilayered construct (Fig. 1L). After 10 days of culture, fibroblasts deposited ECM components, including fibrillar collagens (Fig. 1M, 1N).

hBOEC and hDFS Produce Factors Allowing Communication with Wound Cells

We hypothesized that hBOEC exert trophic effects on healing by producing factors communicating with endogenous vascular and other cell types. As hDFS are thought to synthesize

similar factors, we compared hBOEC and hDFS expression levels with those found in HUVEC. hBOEC expressed higher levels of *VEGF-A*, *PIGF*, *PDGF-B*, *angiopoietin-2* (*Ang-2*), *monocyte/macrophage-chemoattractant protein-1* (*MCP-1*), and *granulocyte/macrophage-colony stimulating factor* (*GM-CSF*), allowing crosstalk with endogenous EC, SMC, and inflammatory cells (Table 1). hBOEC also expressed several *MMP* (*MMP-1*, *-9*, and *-14*) that may modulate collagen metabolism, and, to a comparable extent as HUVEC, *bFGF*. hBOEC expressed factors that stimulate keratinocyte proliferation and migration, including *keratinocyte growth factor* (*KGF*), *interleukin-6*, hepatocyte growth factor (*HGF*), and *GM-CSF* (Table 1). Most strikingly, *KGF* mRNA expression was 280-fold higher in hBOEC compared with HUVEC. Interestingly, hDFS had a distinctly different growth factor expression profile from hBOEC: hDFS did not express *PDGF-B*, *Ang-2*, *GM-CSF* and only minimally *MCP-1* and *PIGF*, but did produce readily detectable levels of *Ang-1* (Table 1). Compared with hBOEC, hDFS expressed \sim 250-fold and \sim 19-fold higher levels of *HGF* and *KGF*, respectively (Table 1). Although *MMP-14* expression was similar in hDFS and hBOEC, the latter secreted slightly more active *MMP-9* (important for their angiogenic properties [33]) than hDFS (Supporting Information Figure S5). Instead, hDFS expressed significantly more mRNA for *MMP-1*, important for fibrillar collagen remodeling (Table 1) [34].

hBOEC, Unlike HUVEC, Induce Wound Vascularization and Re-Oxygenation

Two days after seeding, AcLDL-labeled hBOEC were evenly distributed over the wound (Fig. 2B; Supporting Information Note S5) and detected until day 10, sometimes colocalized with blood-filled vessels (Fig. 2C, 2D). Since UEA-lectin binds hBOEC (Fig. 1G and Supporting Information Figure S6F) but not murine EC (Supporting Information Figure S6E), we used UEA-lectin to quantify hBOEC engraftment. At day 5, 138 ± 23 UEA-lectin⁺ cells per square millimeter ($n = 4$) were detected in the wound bed, some of which participated in the formation of large vessels at the borders (Fig. 2F), whereas others were scattered as single cells in the center (not shown). At day 10, few hBOEC remained. HUVEC were found in the borders at day 5, some of them in hybrid vessels (Supporting Information Figure S6C) or in the wound center in cord-like structures that did not connect with the host vasculature (Supporting Information Figure S6D). In contrast, early EPC did not incorporate into vessels (Fig. 1K).

Two neovascularization peaks were identified by laser doppler analysis—one at day 4, another at day 8—in hBOEC but not in saline-treated wounds (Supporting Information Figure S2). Using species-specific *CD31* antibodies or human-specific UEA-lectin (Supporting Information Figure S6G–J), we observed the formation of functional hybrid vessels containing hBOEC and adjacent murine EC (Fig. 2E). At day 5, vessels were predominantly found at the borders, $8 \pm 1\%$ of which contained hBOEC (Fig. 2F), indicating their significant direct contribution to neovascularization. At day 10, vessels were observed throughout the wound; however, hBOEC were only occasionally found in these (Fig. 2E, 2G). The presence of erythrocytes in hBOEC-derived vessels indicated their functional connection to the host vascular network (Fig. 2E–2G). Based on their expression of angiogenic factors (Table 1), we anticipated that hBOEC would have trophic effects on host vessel network expansion. Indeed, wound edges of hBOEC-treated mice contained twice as much mouse (m)*CD31*⁺ vessels than those of saline-treated mice (Fig. 2H, 2I; Table 2). At day 10, compared with saline, the entire

Table 1. Growth factor expression profile of hBOEC and hDFS

	HUVEC (P4) ^a		hBOEC (P4) ^a		hDFS ^a	
	RNA	Protein	RNA (%)	Protein	RNA (%)	Protein
Communication with vascular/inflammatory cells						
VEGF-A	100	ND	204 ± 13 ^b	ND	199 ± 78 ^c	ND
PIGF	100	1,800 ± 160	300 ± 37 ^b	3,300 ± 160 ^b	3 ± 1 ^{b,d}	7 ± 2 ^d
PDGF-BB	100	<1.4	259 ± 14 ^b	46 ± 18	0 ± 0 ^{b,d}	0 ± 0 ^d
Angiopoietin-1	100	ND	0 ± 0 ^b	ND	855 ± 50 ^{b,d}	ND
Angiopoietin-2	100	ND	861 ± 107 ^b	ND	0 ± 0 ^{b,d}	ND
MCP-1	100	ND	293 ± 59 ^b	ND	4 ± 1 ^{b,d}	ND
bFGF	100	ND	169 ± 81	ND	65 ± 3 ^b	ND
Communication with fibroblasts (matrix)						
MMP-9	100	ND	ND	Supporting Information Fig. S5	ND	Supporting Information Fig. S5
MMP-14	100	ND	73 ± 9	ND	85 ± 6	ND
MMP-1	100	ND	218 ± 18 ^b	ND	7,684 ± 560 ^{b,d}	ND
Communication with keratinocytes (proliferation/migration)						
KGF	100	0 ± 0	28,000 ± 3,000 ^b	2 ± 1 ^b	525,000 ± 88,000 ^{b,d}	23 ± 3 ^{b,d}
Interleukin-6	100	ND	63 ± 10	ND	26 ± 17 ^b	ND
HGF	100	ND	132 ± 43	ND	34,000 ± 7,000 ^{b,d}	ND
GM-CSF	100	ND	6,000 ± 900 ^b	ND	0 ± 0 ^{b,d}	ND

RNA data represent mean (±SEM) of three to five independent isolations, determined by qRT-PCR and expressed as % versus HUVEC and normalized to β -actin. Protein data represent mean (±SEM) of three independent supernatant samples, determined by ELISA and expressed as picogram per milligram protein; Statistical comparisons were performed on the absolute (not relative to HUVEC) expression data; ^aGene/protein levels were determined on cells incubated in normoxia (20% O₂); ^b $p < 0.05$ and ^c $p = 0.08$ versus HUVEC; ^d $p < 0.05$ versus hBOEC.

Abbreviations: bFGF, basic fibroblast growth factor; GM-CSF, granulocyte/macrophage-colony stimulating factor; hBOEC, human blood outgrowth endothelial cells; hDFS, human dermal fibroblast sheets; HGF, hepatocyte growth factor; HUVEC, human umbilical vein endothelial cells; KGF, keratinocyte growth factor; MCP-1, monocyte/macrophage-chemoattractant protein-1; MMP, matrix metalloprotease; ND, not determined; P, passage; PDGF, platelet-derived growth factor; PIGF, placental growth factor; VEGF, vascular endothelial growth factor.

wound contained more mCD31⁺ vessels when seeded with hBOEC (Fig. 2J, 2K; Supporting Information Figure S7; Table 2). Interestingly, dose-response studies revealed that tripling the hBOEC dose increased vessel density (mCD31⁺ vessel number/mm²: 376 ± 39 for 1.5 × 10⁶ hBOEC vs. 271 ± 27 for 5 × 10⁵ hBOEC; $n = 4-6$; $p < .05$; Supporting Information Figure S8A,B). HUVEC transplantation did not increase the mCD31-positive area fraction compared with saline-treated wounds (Table 2).

Since hBOEC secreted PIGF and PDGF-BB, factors that have chemoattractive and/or proliferative effects on SMC [35, 36], we determined whether hBOEC increased the number of SMC-coated vessels. At day 5, the borders of hBOEC-treated wounds contained twice the amount of smooth muscle cell-actin (SMA)-coated vessels compared with wounds from the saline group or HUVEC (Fig. 2L, 2M; Table 2). The center of hBOEC-treated wounds also contained more SMA⁺ vessels than the saline-infused wounds at day 10 (265 ± 22 vs. 179 ± 16; $n = 5$; $p < .05$; Fig. 2N, 2O).

Since wound revascularization is supposed to relieve hypoxia, we tested whether the hBOEC-induced vascular expansion decreased the amount of hypoxic cells in the wound. Therefore, a separate set of animals was injected with HypoxyprobeTM and hypoxic cells were traced by immunohistochemistry [8]. hBOEC treatment reduced the hypoxic cell fraction by ~40% (% hypoxic cells: 24 ± 1 in saline-treated vs. 15 ± 1 in hBOEC-treated wounds; $n = 5$; $p < .05$; Fig. 2P-2R). Moreover, the decrease in hypoxic cell fraction inversely correlated with the area taken up by blood vessels ($R^2 = 0.545$; $p < .05$; Fig. 2U) and hypoxic cells mainly resided in avascular areas (Fig. 2P, 2Q, 2S, 2T).

hBOEC, Unlike HUVEC, Enhance Matrix Organization and Accelerate Epithelial Coverage

In a next step, we evaluated epithelialization and collagen deposition/organization. Compared with saline or HUVEC, hBOEC transplantation increased the epithelialization at day 5 (Fig. 3A, 3B; Table 2). The fraction of migrating keratinocytes, detected by downregulation of connexin43 (ref. [37]), was higher in the presence of hBOEC (Fig. 3C, 3D; Table 2). At day 10, all hBOEC-treated wounds were re-epithelialized completely, while re-epithelialization was only 87 ± 4% in the saline group (Table 2). To evaluate fibrillar collagen deposition and organization, we analyzed SRed-stained sections under bright and polarized light, respectively [30]. The presence of hBOEC did not increase deposition (% fibrillar collagen; Table 2) but, unlike HUVEC, improved organization at day 10 (% red-birefringent collagen; Fig. 3E, 3H; Table 2). This improvement was confirmed by examining collagen bundling on semi-thin sections (Fig. 3F, 3I) and at the ultrastructural level on transmission electron micrographs (Fig. 3G, 3J). Interestingly, the percentage organized collagen was ~2-fold higher with higher hBOEC dose (Supporting Information Figure S8C,D).

O₂ and hBOEC-Conditioned Medium Stimulate hDFS and Keratinocyte Behavior

As increased vascularization by hBOEC improved wound oxygenation, we studied the effect of oxygen levels on hDFS and keratinocytes. hDFS or keratinocytes were cultured in hypoxic (1% O₂; Supporting Information Note S6) or normoxic (20% O₂) conditions for 10 days (the duration of our in vivo experiment). Increased oxygen levels resulted in increased organization of fibrillar collagen deposited by hDFS

Table 2. Early and late effects of hBOEC, HUVEC, hDFS, and hDFS + hBOEC on wound healing

	PBS	HUVEC	hBOEC	hDFS	hDFS + hBOEC
<i>Wound revascularization and closure in early phase (day 5)</i>					
Wound revascularization; <i>N</i> = 6–12					
mCD31 ⁺ area fraction (%) ^a	6 ± 1	5 ± 1	12 ± 1 ^{b,d}	10 ± 1 ^b	13 ± 1 ^{b,c}
No. α-SMA ⁺ vessels/mm ²	97 ± 11	87 ± 11	208 ± 29 ^{b,d}	205 ± 26 ^b	180 ± 15 ^b
Wound closure; <i>N</i> = 6–12					
% Contraction (day 4)	22 ± 3	25 ± 4	21 ± 7	17 ± 4	21 ± 4
Myofibroblast area fraction (%)	3.8 ± 0.4	5.0 ± 2.0	3.3 ± 1.0	0.7 ± 0.3 ^b	0.4 ± 0.1 ^b
Epidermal closure					
% Epithelial coverage ^f	14 ± 3	19 ± 3	31 ± 7 ^{b,e}	60 ± 14 ^b	43 ± 10 ^b
No keratinocytes/mm ² ^g	410 ± 40	ND	410 ± 30	440 ± 30	590 ± 40 ^{b,c}
% Connexin43 ^{low} keratinocytes	59 ± 3	57 ± 2	74 ± 6 ^{b,d}	ND	ND
<i>Wound revascularization, closure, and matrix organization in late phase (day 10)</i>					
Wound revascularization; <i>N</i> = 6–11					
mCD31 ⁺ area fraction (%) ^h	6 ± 1	5 ± 1	25 ± 5 ^{b,d}	10 ± 3	24 ± 5 ^{b,c}
Wound closure					
% Contraction; <i>N</i> = 6–12	81 ± 3	84 ± 3	79 ± 4	67 ± 5 ⁱ	59 ± 8 ^j
Epidermal closure					
% Epithelial coverage ^f ; <i>N</i> = 6–23	87 ± 4	94 ± 3	99 ± 1 ^b	98 ± 4 ^b	100 ± 0 ^b
Epithelial thickness (μm) ^k ; <i>N</i> = 7–11	66 ± 6	ND	53 ± 6	47 ± 8	98 ± 13 ^{b,c}
Wound matrix organization; <i>N</i> = 6–15					
% Fibrillar collagen	58 ± 3	62 ± 3	63 ± 3	67 ± 3 ^b	71 ± 2 ^{b,l}
% Red-birefringent collagen	28 ± 3	28 ± 3	47 ± 2 ^{b,d}	32 ± 3	48 ± 5 ^c
Data represent mean (±SEM).					
^a % of total area in wound borders.					
^b <i>p</i> < 0.05 versus PBS.					
^c <i>p</i> < 0.05 versus hDFS.					
^d <i>p</i> < 0.05 versus HUVEC.					
^e <i>p</i> = 0.06 versus HUVEC.					
^f % of total wound length, defined as the distance between the two first appearing hair follicles.					
^g Counted in the advancing epithelial edges.					
^h % of total area in entire wound bed.					
ⁱ <i>p</i> = 0.07 versus saline.					
^j <i>p</i> < 0.05 versus hBOEC.					
^k Average thickness determined over the entire wound length.					
^l <i>p</i> = 0.05 versus saline.					
Abbreviations: hBOEC, human blood outgrowth endothelial cells; hDFS, human dermal fibroblast sheets; ND, not determined; PBS, phosphate-buffered saline; SMA, smooth muscle cell actin.					

(% red-birefringent collagen: 13 ± 3 at 1% O₂ vs. 32 ± 2 at 20% O₂; *n* = 4; *p* < .005; Fig. 4A, 4B, 4D), further confirmed by semi-thin sections (Fig. 4E, 4F). Interestingly, under hypoxic conditions, hDFS expressed twofold more mRNA encoding MMP-1, the main MMP responsible for fibrillar collagen degradation (Supporting Information Figure S3H) [34]. Keratinocytes migrated more slowly after long-term exposure to hypoxia, as revealed in a scratch wounding assay [area covered by migrating keratinocytes in a 1-mm window 24 hours after wounding (μm² × 10⁵): 2.8 ± 0.4 at 1% O₂ vs. 5.1 ± 0.3 at 20% O₂; *n* = 4; *p* < .05; Fig. 4I, 4J, 4M]. In agreement, qRT-PCR revealed that 24 hours after wounding, keratinocytes expressed threefold more *connexin43* in hypoxia (*n* = 3; *p* < .05; Supporting Information Figure S3G), corresponding to a less migratory phenotype [37]. In addition, lowering oxygen levels also significantly decreased keratinocyte proliferation by a factor of 1.5 (*n* = 4–6; *p* < .005; Fig. 4N, 4O, 4R).

hBOEC communicate with fibroblasts and keratinocytes via secreted factors known to influence dermal organization or keratinocyte migration/proliferation (Table 1) [1, 2]. Collagen produced by hDFS cultured in hBOEC-conditioned media was significantly more organized compared with NCM (% red-birefringent collagen: 32 ± 2 in the absence vs. 51 ± 2 in the presence of hBOEC-conditioned media; *n* = 4; *p* < .005; Fig. 4B–4D; confirmed on semi-thin sections and by TEM; Fig. 4F–4H) suggesting a paracrine effect of hBOEC

on hDFS. In addition, hBOEC-conditioned media contained factors that boosted keratinocyte migration [area covered by migrated keratinocytes in a 1-mm window 6 hours after wounding (μm² × 10⁵): 2.8 ± 0.3 with hBOEC-conditioned media vs. 1.9 ± 0.3 with NCM; *n* = 4; *p* < .05; Fig. 4K–4M] and proliferation (keratinocyte number × 10³ per square centimeter after 10 days: 74 ± 6 with hBOEC-conditioned media vs. 51 ± 6 with NCM; *n* = 4; *p* < .05; Fig. 4P–4R). In accordance, keratinocytes had a more migratory phenotype [37] in the presence of hBOEC-conditioned media, shown by their 2.3-fold lower *connexin43* expression compared with NCM (*n* = 4; *p* < .05; Supporting Information Figure S3G).

hBOEC-Derived PIGF Mediates hBOEC and Keratinocyte but not hDFS Behavior

Since PIGF was abundantly produced by hBOEC, and fibroblasts and keratinocytes expressed its receptor Flt-1 (Supporting Information Figure S9A), we hypothesized that the effects of hBOEC were at least partially mediated by PIGF. Using an shRNA-encoding lentivirus, PIGF was successfully knocked-down, shown by a dramatic decrease in PIGF protein in the supernatant (Supporting Information Figure S9B). Although knocking-down PIGF in hBOEC did not significantly change their expression of endothelial markers or other growth factors (Supporting Information Note S7), it decreased their

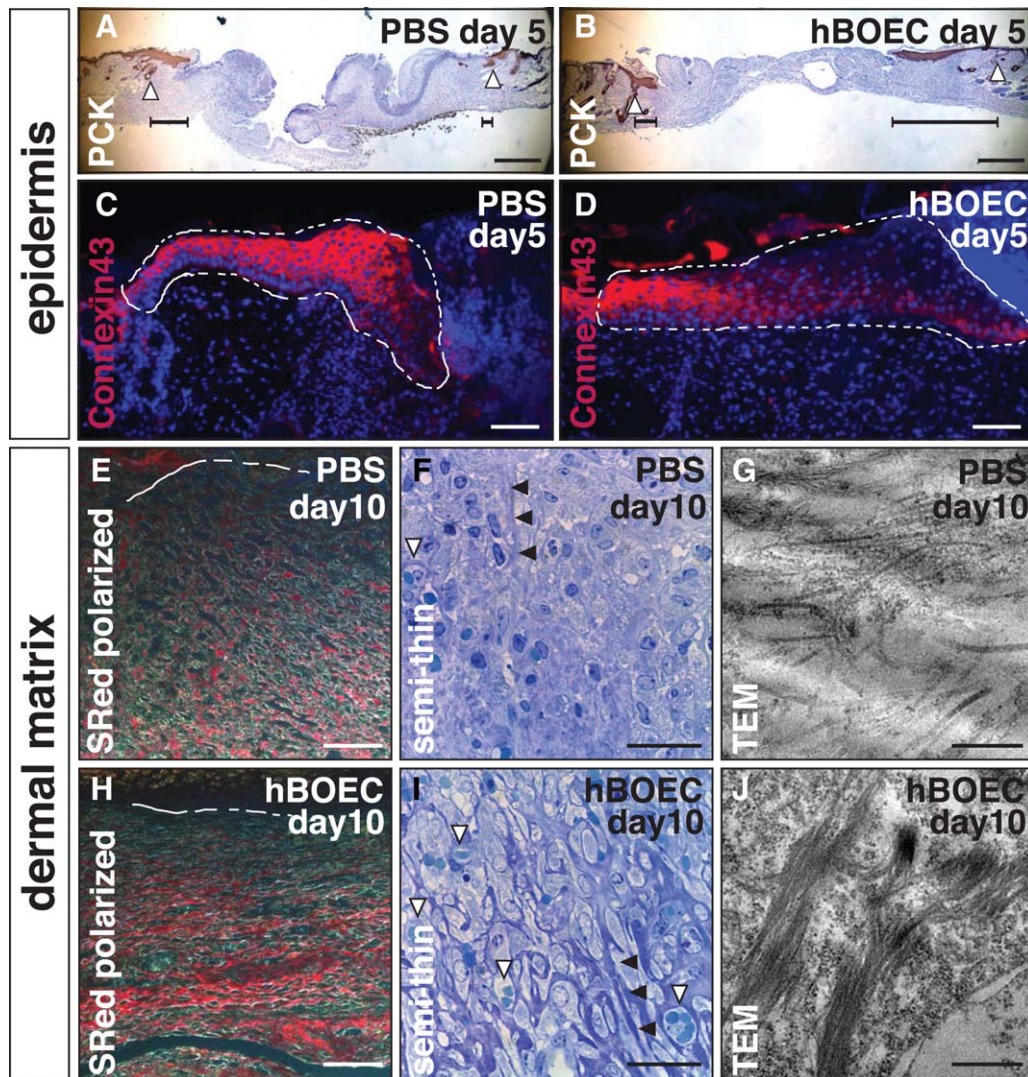


Figure 3. hBOEC enhance matrix organization and re-epithelialization of wounds. (A, B): The epidermal front (revealed by PCK) moved faster over the wound in hBOEC-treated (B) compared with PBS-treated wounds (A). Hair follicles marking wound boundaries and the length covered by the epidermis are indicated by white arrowheads and black lines, respectively. (C, D): Cross-sections stained with connexin43 in red showing more migrating (i.e., cells that have downregulated connexin43) keratinocytes in the epidermal tongue (indicated by white-dashed lines) of hBOEC-treated (D) versus PBS-treated (C) wounds. (E–J): Collagen organization was analyzed by Sirius-red polarization microscopy (E, H), on semi-thin sections (F, I) and by TEM (G, J), revealing that collagen was more aligned in thick bundles [shown by the red birefringence, the thicker blue matrix structures (indicated by black arrowheads) on semi-thin sections and the parallel positioning of the collagen fibers on TEM] in hBOEC-treated (H–J) compared with PBS-treated (E–G) wounds. 4',6-diamino-2-phenylindole (DAPI) (blue) was used as nuclear counterstaining in (C, D). The dermoepidermal junction is indicated by white-dashed lines in (E, H) and blood vessels by white arrowheads in (F, I). Scale bars: 0.5 μm in (G, J), 25 μm in (F, I), 50 μm in (E, H), 75 μm in (C, D), and 500 μm in (A, B). Abbreviations: hBOEC, human blood outgrowth endothelial cells; PBS, phosphate-buffered saline; PCK, pancytokeratin; TEM, transmission electron microscopy.

proliferation (Supporting Information Figure S9C), suggesting a role for PIGF as an autocrine mitogen. Increasing or lowering PIGF exposure to hDFS did not alter collagen organization (not shown). However, PIGF^{KD}-BOEC conditioned media significantly decreased keratinocyte proliferation (Supporting Information Figure S9D) and migration in a scratch wound assay (Fig. 4S, 4T, 4W). Accordingly, adding rhPIGF to keratinocyte cultures increased their proliferation and migration (Fig. 4U–4W and Supporting Information Figure S9D).

hBOEC Improve Matrix Organization and Re-Epithelialization of hDFS in Wounds

Wound contraction significantly hampers mobility in joint regions and leads to unaesthetic scars [38]. We used a multi-

layered fibroblast construct (Fig. 1L–1N) and assessed whether it would prevent contraction (Supporting Information Note S2). Although hBOEC alone did not reduce contraction, the presence of hDFS—singly or combined with hBOEC—significantly decreased contraction near the end of the healing period (Fig. 5A, 5B; Table 2). Reduced contraction was accompanied by a decrease in the area taken up by SMA-expressing myofibroblasts at the wound edges 5 days after wounding (Fig. 5C–5F; Table 2). In addition, the presence of hDFS—singly or combined with hBOEC—significantly increased collagen deposition at 10 days, compared with the corresponding conditions without hDFS (% fibrillar collagen; Table 2). Finally, filling the wound gap with hDFS—singly or combined with hBOEC—had markedly increased the epithelialization rate at 5 days compared with saline (Figs. 3A, 5G, 5H; Table 2). At 10 days, wounds containing hDFS and

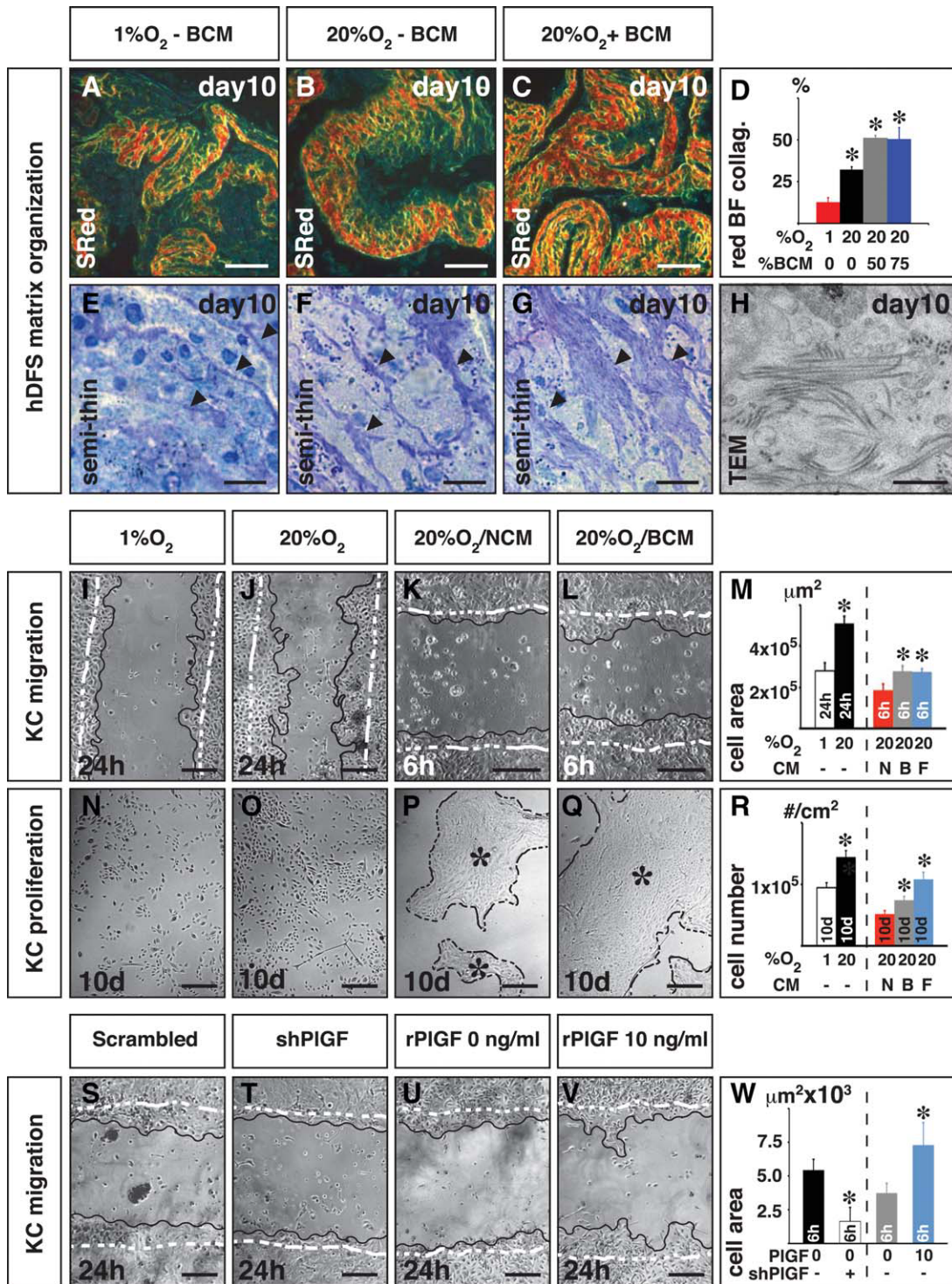


Figure 4. O₂, hBOEC-CM, and PIGF modulate hDFS and/or keratinocyte behavior in vitro. (A–D): SRed-stained cross-sections (viewed under polarized light) of hDFS in 1% O₂ without BCM [(A), red bar in (D)] or 20% O₂ in the absence [(B), black bar in (D)] or presence [(C), gray and blue bar in (D)] of BCM, revealing more organized [i.e., red-birefringent collagen; red BF collag.; % vs. total area in (D)] collagen in 20% O₂, further increased by BCM. (E–H): Semi-thin sections (E–G) and transmission electron micrograph (H) revealing thicker collagen bundles [black arrowheads in (E–G)] in normoxia (F) compared with hypoxia (E) and even more thick bundles in the presence of BCM (G, H). (I–M): Wounding assay revealing more migrating KC [area in square micrometer occupied by migrating KC in a 1-mm window in (M)] at 24 hours in normoxia [(J); black bar in (M)] versus hypoxia [(I); white bar in (M)]. Migration was also increased with BCM [(L); “B” and gray bar in (M)] compared with NCM [(K); “N” and red bar in (M)]. Moreover, hDFS-CM [(F) and blue bar in (M)] also increased KC migration. (N–R): Proliferation assay of KC grown in normoxia [(O); black bar in (R)] or hypoxia [(N); white bar in (R)] revealing more cell expansion in normoxia [number of cells per square centimeter in (R)]. In addition, BCM [(Q); “B” and gray bar in (R)], and even more so, hDFS-CM [(F) and blue bar in (R)] increased KC proliferation compared with NCM [(P); “N” and red bar in (R)]. *, *p* < .05 versus hypoxia or NCM. (S–W): Wounding assay revealing less migrating KC [area in square micrometer occupied by migrating KC in a 1-mm window at 6 hours in (W) or at 24 hours in (S–V)] in the presence of 50% conditioned media from hBOEC treated with shPIGF [(T); white bar in (W)] when compared with 50% conditioned media from hBOEC treated with scrambled shRNA [(S), black bar in (W)]. Migration was however increased in KC growth media supplemented with 10 ng/ml PIGF [(V), blue bar in (W)] when compared with without supplemented PIGF [(U), gray bar in (W)]; *, *p* < .05; *n* = 4. Original wound is indicated by dashed white lines and the moving KC front by wavy black lines in (I–L) and (S–V). Scale bars: 1 μm in (H), 10 μm in (E–G), 50 μm in (A–C), and 300 μm in (I–L, N–Q, S–V). Abbreviations: BCM, hBOEC-conditioned media; BF, birefringent; CM, conditioned media; hBOEC, human blood outgrowth endothelial cells; hDFS, human dermal fibroblast sheets; NCM, nonconditioned media; PIGF, placental growth factor; KC, keratinocytes; SRed, Sirius-red; TEM, transmission electron microscopy.

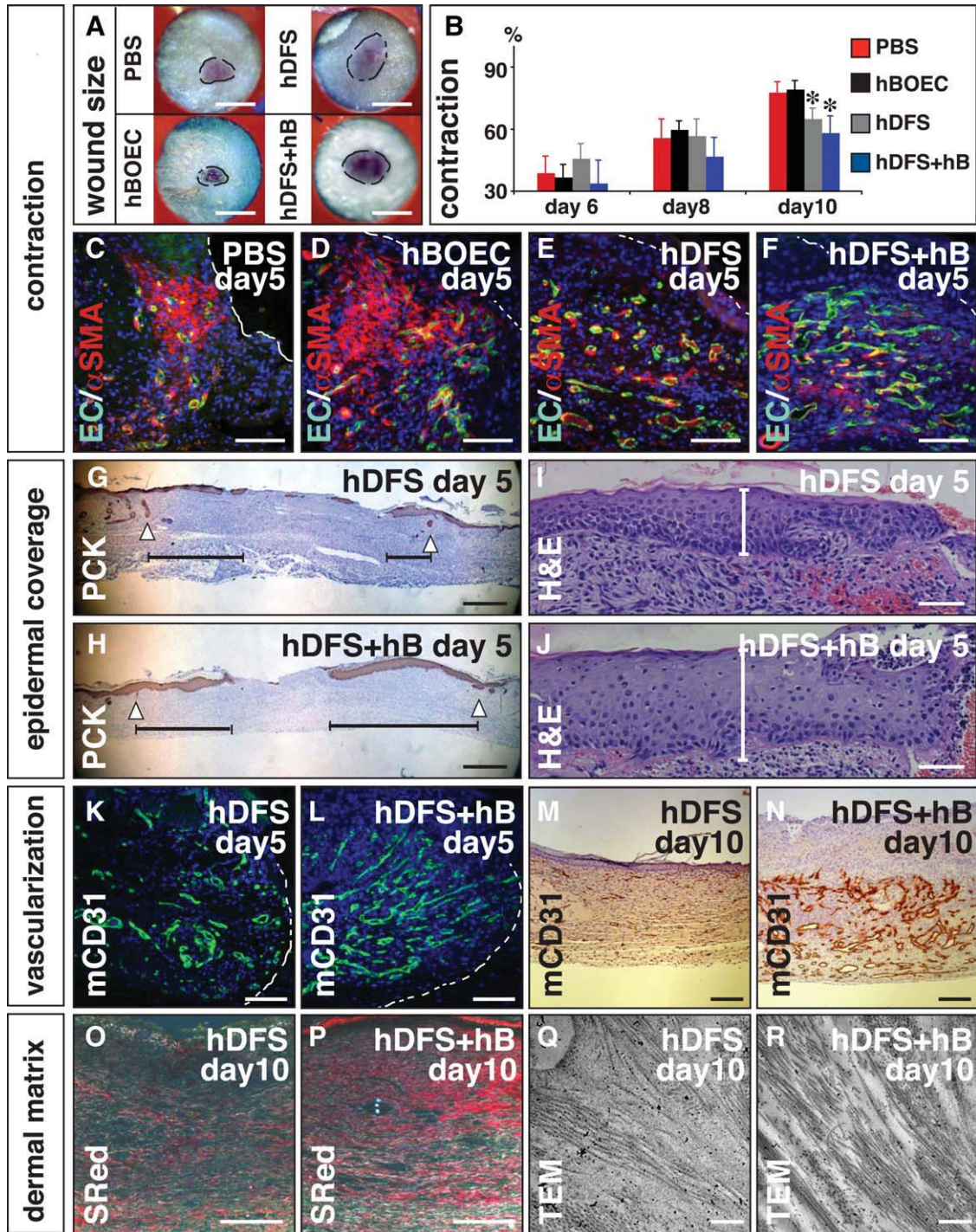


Figure 5. hBOEC improve hDFS vascularization, matrix organization, and re-epithelialization. (A, B): Size (A) and contraction [% relative to original wound size in (B)] in wounds treated with PBS [red bars in (B)], hBOEC [black bars in (B)], hDFS [gray bars in (B)], or hBOEC + hDFS [blue bars in (B)] revealing reduced contraction in conditions with hDFS. (C–F): Cross-sections of PBS (C), hBOEC (D), hDFS (E), or hBOEC (hB) + hDFS (F) treated wounds double-stained for EC [mouse and human, using mouse-specific CD31, and human-specific Ulex Europaeus Agglutinin (UEA)-lectin in green] and SMC (revealed by red SMC- α -actin) showing less myofibroblasts (corresponding to SMC- α -actin⁺ signal not associated with green EC) at the wound edges in conditions with hDFS. (G, H): Cross-sections of wounds treated with hDFS alone (G) or combined with hBOEC (H) stained with PCK revealing faster epithelial coverage in conditions with hDFS compared with PBS-treated wounds (see Fig. 3A). Hair follicles marking wound boundaries and the length covered by epidermis are indicated by white arrowheads and black lines, respectively. (I, J): Cross-sections stained with H&E revealing that the epithelial tongue has an increased thickness (indicated by white lines) in hBOEC containing hDFS (J) than in hDFS alone (I). (K–N): Cross-sections of wound borders at day 5 [stained with green mouse-specific CD31 in (K, L)] and wound centers at day 10 [stained with mouse-specific CD31 in (M, N)] revealing more vessels in hDFS combined (L) or not (K) with hBOEC when compared with PBS-treated wounds at day 5 (see Fig. 2H). At day 10, hBOEC increased vascularization of hDFS in the wound center [(N) vs. (M)]. (O–R): Collagen, analyzed by SRed polarization microscopy (O, P) and TEM (Q, R), was more aligned in thick bundles in hDFS + hBOEC-treated (P, R) compared with hDFS alone (O, Q) wounds. 4',6-diamino-2-phenylindole (DAPI) (blue) was used as nuclear counterstaining in (C–F) and (K, L). Wound edges are lined by white-dashed lines in (C–F) and (K, L). Scale bars: 0.5 μ m in (Q, R), 75 μ m in (C–F, I, J, O, P), 200 μ m in (K–N), 500 μ m in (G, H), and 3 mm in (A). Abbreviations: SMA, smooth muscle cell-actin; EC, endothelial cells; H&E, hematoxylin and eosin; hBOEC, human blood outgrowth endothelial cells; hDFS, human dermal fibroblast sheets; PBS, phosphate-buffered saline; PCK, pancytokeratin; SRed, Sirius-red; TEM, transmission electron microscopy.

hDFS + hBOEC were significantly more re-epithelialized than those in the saline group (Table 2). Growth factor analysis (Table 1) and keratinocyte proliferation/migration assays in the presence of hDFS-conditioned media (Fig. 4M, 4R) further support the notion that improved epithelial coverage is related to crosstalk of fibroblasts and keratinocytes. In accordance, keratinocytes had a more migratory phenotype in the presence of hDFS-conditioned media, as shown by their 1.3-fold lower expression of *connexin43* compared with NCM ($n = 4$; $p < .05$; Supporting Information Figure S3G) [37].

Next, we assessed whether hBOEC increased vascularization of hDFS in wounds. At day 5, compared with saline, the presence of hDFS alone was sufficient to increase the number of mCD31⁺ vessels in the borders, likely by a trophic effect (Table 1) on angiogenesis. Addition of hBOEC further increased this trophic effect (Fig. 5K, 5L; Table 2). The presence of hDFS alone was also sufficient to increase the number of SMA-coated vessels, an effect that was not further enhanced by hBOEC (Table 2). At 10 days, vessels occupied the entire wound, including the hDFS. Although at this stage hDFS alone did no longer increase vascularization when compared with saline, the presence of hBOEC did enhance vascularization of the entire wound (mCD31⁺ area fraction; Figs. 2J, 5M, 5N; Table 2).

Finally, we investigated whether hBOEC-mediated neovascularization of hDFS was consistent with our in vitro findings at increased oxygen levels. Although hBOEC did not affect collagen deposition (% fibrillar collagen; Table 2), they did improve collagen organization within hDFS implanted in wounds (% red-birefringent collagen; Fig. 5O, 5P; Table 2). This increased organization was confirmed by TEM (Fig. 5Q, 5R) and on semi-thin sections (Supporting Information Figure S10). Consistent with the observed in vitro effect of increased oxygen levels on keratinocyte proliferation, hBOEC increased the number of keratinocyte layers in the advancing epithelial tongues at 5 days on top of the implanted hDFS (keratinocyte number per millimeter: 590 ± 40 in hDFS + hBOEC vs. 440 ± 30 in hDFS; $n = 6$; $p < .05$; Fig. 5I, 5J). Moreover, at day 10, the epithelium covering the hDFS was thicker in the presence of hBOEC (epithelial thickness; Table 2). Interestingly, under low oxygen conditions, hDFS secreted significantly less of the keratinocyte proliferation factor KGF when compared with normoxic conditions (picogram per milligram protein: 14 ± 1 in hypoxia vs. 23 ± 3 in normoxia; $n = 4$; $p < .05$).

DISCUSSION

Sufficient vascularization is quintessential for wound healing and crucial for ingrowth of skin substitutes [27]. We explored the effect of hBOEC singly or combined with a human dermal fibroblast construct on vascularization in wound healing. hBOEC improved vascularization and—consequently—oxygenation by direct incorporation into the host vasculature, and via trophic expansion of the host vessel network. The result was faster re-epithelialization and better matrix organization. Integration of hBOEC in a multilayered fibroblast construct further promoted blood vessel growth, leading to more extensive epithelial coverage and improved matrix organization. In addition, the presence of hDFS reduced wound contraction. Our in vitro studies suggested that the effects of hBOEC on re-epithelialization and matrix organization were at least partly due to the re-oxygenation of the wound bed as well as to the growth factor crosstalk with surrounding wound cells, that is, keratinocytes and fibroblasts. PlGF was responsible for

some of these effects. All of these cells can be harvested from the host and thus offer the possibility of an entirely autologous and safe approach to tissue-engineering for wound repair.

Most current cell-related wound vascularization strategies focus on MSC [22, 23]. However, they may cause excessive contraction by differentiating into myofibroblasts [39]. Moreover, direct vascular contribution of MSC is debated [40, 41]. We opted for peripheral blood-derived hBOEC as a source of new vessels and showed that, despite their endothelial signature and function resembling that of mature EC [18], both cell types have several distinct characteristics. Indeed, a thorough characterization of hBOEC involves documentation of their differential behavior not only from early EPC but also mature EC. We determined for the first time that the latter difference concerns their proliferative behavior, as well as other functional aspects, including, for example, secretion of MMP and growth factors. Although others suggested that hBOEC do not contribute to vascularization by secreting growth factors, these investigators restricted their assays to an in vitro transwell system [12]. We demonstrate an important trophic role for hBOEC in vessel growth in vivo where cell-cell contact is critical for optimizing this crosstalk. The difference between mature EC and hBOEC is further underscored by the fact that, unlike hBOEC, mature EC do not efficiently contribute to neovascularization in wounds and ischemic hind limbs [17, 18]. We acknowledge that instead of HUVEC, circulating EC would be the ideal reference population for our comparative studies, however, obtaining these in sufficient numbers represents a technical barrier. Intriguingly, although a significant number of hBOEC were present at 5 days, they had mostly disappeared by day 10. This temporary presence was however sufficient to sustain the effect on revascularization, perhaps due to a prolonged effect of the trophic factors they released.

Except for cord blood-derived BOEC, unavailable for most patients, peripheral blood is the only readily accessible autologous source of BOEC. Although cord blood-BOEC have the advantages of higher proliferation and vascularization capacity [42], recent evidence suggests that this can be compensated for by preconditioning of peripheral blood-derived BOEC with angiogenic growth factors [43]. In addition, the more proliferative nature of cord blood-BOEC may cause cytogenetic abnormalities, which were not observed in peripheral blood-BOEC [44]. The need for exogenously added BOEC is underscored by the observation that the contribution of endogenous EC precursors is insignificant during wound vascularization [45]. Although allogeneic BOEC are more easily available, they have the capacity to initiate an immune response by resting allogeneic T-lymphocytes [46], necessitating the use of autologous BOEC. Autologous fibroblasts may however also be advantageous over allogeneic sources, since the latter were documented to increase scar formation and wound contraction [47].

Early wound healing studies [4] and our current measurements have shown that the wound bed is severely hypoxic, a situation not compatible with the high metabolic demands of the cells involved in repair. Although acute hypoxia is a necessary trigger to initiate many aspects of the healing process, prevention of long-term hypoxia by re-oxygenation should be an important goal for every wound healing approach. Although many revascularization therapies have merely suggested a link between revascularization and re-oxygenation, here we directly demonstrated that hBOEC-induced revascularization inversely correlated to the extent of hypoxia. The deleterious effect of long-term hypoxia on wound cell behavior was further tested by exposing the cells to high or low

oxygen for at least 10 days. Keratinocyte migration and proliferation were compromised by sustained low oxygen levels. These results appear to be in conflict with earlier studies. However, those studies evaluated the effect of acute hypoxia on keratinocytes, which may indeed be stimulatory instead of inhibitory [48]. The role of oxygen in collagen fibrillogenesis has been previously documented [5]. Sustained hypoxia also significantly hampered collagen organization. Again, the effect of hypoxia on fibroblasts can vary, depending on the duration of the hypoxia [7]. The underlying molecular mechanisms by which oxygen tension regulates matrix organization are incompletely understood. The expression and activity levels of the key matrix-modulating factors, the MMP, may be affected by changes in oxygen levels. Indeed, we and others have shown in a three-dimensional fibroblast culture that MMP-1 levels are upregulated by hypoxia [49].

Several fibroblast-containing dermal substitutes, with or without keratinocytes, have been approved for clinical use (e.g., Dermagraft, Apligraf, Orcel) [3]. All of these rely on an artificial matrix to deliver fibroblasts. We tried to mimic the composition of natural dermis by superimposing several dermal fibroblast sheets, allowing them to produce their own ECM over time. Ultrastructural analysis and histology indeed revealed that these hDFS produced their own collagen matrix, the organization of which could be improved by increasing oxygen levels and adding hBOEC-conditioned media. Exactly which factors in hBOEC-conditioned media are responsible for this improved organization remains to be determined. Although transforming growth factor (TGF)- β 1 was suggested as a potential "organizer" [50], hBOEC did not synthesize this factor in measurable amounts (not shown). They did however produce PDGF-BB, although there is no consensus on whether this factor improves collagen organization [50, 51]. Perhaps, MMP-9 expression by hBOEC contributed to collagen organization, since a lack of this MMP results in disordered fibrillogenesis [52]. hBOEC abundantly produce PIGF. Although this factor has been shown to stimulate fibroblast migration [25], here we did not find an effect on collagen organization. Instead PIGF significantly induced keratinocyte migration and proliferation. Interestingly, analysis of the growth factor expression pattern suggested that hDFS produced a spectrum of factors that was often complementary and potentially synergistic to that of hBOEC. Accordingly, effects on wound healing parameters were most prominent and complemented each other when hDFS and hBOEC were combined. For example, although hDFS boosted collagen deposition, hBOEC promoted collagen organization so that the texture of collagen fibers started to closely resemble the basket-weave pattern typical for normal skin. A causal link between myofibroblasts and wound contraction has been previously suggested [38]. In our model, the presence of hDFS inhibited contraction in the later phases of wound closure and

this correlated with a reduction in myofibroblast content at the wound edges (Table 2).

On the basis of our *in vitro* experiments, we proposed that the beneficial effect of hBOEC on wound healing is mediated by growth factor crosstalk and better oxygenation through vascularization. Which of these two mechanisms is (most) active for each of the wound healing processes *in vivo* is difficult to dissect. Although adding a growth factor combination to the wound bed could reveal the importance of the trophic effect, this may be underestimated since the bioavailability could be different when cells deliver growth factors in a continuous way to the wound. Nevertheless, the knockdown experiments underscore the importance of PIGF in re-epithelialization. On the other hand, using a higher hBOEC dose revealed that collagen organization correlated with vascular density, suggesting a link between these two processes.

CONCLUSION

In conclusion, using a murine wound healing model, we have provided strong evidence that hBOEC are effective in increasing vessel formation and accelerating wound healing. The integration of hBOEC in hDFS forms a solid basis for the development of a fully autologous tissue-engineered skin construct suitable for clinical use in patients with large skin defects that do not heal properly. Furthermore, some of the principal underlying mechanisms to the success of this approach were unveiled.

ACKNOWLEDGMENTS

We thank P. Vandervoort, T. Vervoort, V. Claus, B. Hoekman, and T. Koninckx for technical assistance, B. Jordan and B. Gallez for oximetry experiments (UCL, Brussels, Belgium), H. Heimberg, Y. Heremans, S. Bonné, and L. Baeyens (VUB, Belgium) for providing the lentiviral constructs and M. Garmyn (Laboratory of Dermatology, KULeuven, Belgium) for providing keratinocytes. This work was supported by grants from the European Commission (FP7-StG-IMAGINED 203291; A.L.), FWO (post-doctoral fellowship, A.L.; pre-doctoral fellowships, B.H., S.VdB), and a KULeuven Center of Excellence Grant (EF/05/013; A.L.).

DISCLOSURE OF POTENTIAL CONFLICTS OF INTEREST

The authors indicate no potential conflict of interest.

REFERENCES

- 1 Werner S, Krieg T, Smola H. Keratinocyte-fibroblast interactions in wound healing. *J Invest Dermatol* 2007;127:998–1008.
- 2 Hughes CC. Endothelial-stromal interactions in angiogenesis. *Curr Opin Hematol* 2008;15:204–209.
- 3 Wong T, McGrath JA, Navsaria H. The role of fibroblasts in tissue engineering and regeneration. *Br J Dermatol* 2007;156:1149–1155.
- 4 Hunt TK, Twomey P, Zederfeldt B et al. Respiratory gas tensions and pH in healing wounds. *Am J Surg* 1967;114:302–307.
- 5 Rodriguez PG, Felix FN, Woodley DT et al. The role of oxygen in wound healing: A review of the literature. *Dermatol Surg* 2008;34:1159–1169.
- 6 Velazquez OC. Angiogenesis and vasculogenesis: Inducing the growth of new blood vessels and wound healing by stimulation of bone marrow-derived progenitor cell mobilization and homing. *J Vasc Surg* 2007;45 (Suppl A):A39–A47.
- 7 Steinbrech DS, Longaker MT, Mehrara BJ et al. Fibroblast response to hypoxia: The relationship between angiogenesis and matrix regulation. *J Surg Res* 1999;84:127–133.
- 8 Lokmic Z, Darby IA, Thompson EW et al. Time course analysis of hypoxia, granulation tissue and blood vessel growth, and remodeling in healing rat cutaneous incisional primary intention wounds. *Wound Repair Regen* 2006;14:277–288.
- 9 Luttun A, Carmeliet G, Carmeliet P. Vascular progenitors: From biology to treatment. *Trends Cardiovasc Med* 2002;12:88–96.
- 10 Asahara T, Murohara T, Sullivan A et al. Isolation of putative progenitor endothelial cells for angiogenesis. *Science* 1997;275:964–967.

- 11 Yoder MC, Mead LE, Prater D et al. Redefining endothelial progenitor cells via clonal analysis and hematopoietic stem/progenitor cell principals. *Blood* 2007;109:1801–1809.
- 12 Sieveking DP, Buckle A, Celermajer DS et al. Strikingly different angiogenic properties of endothelial progenitor cell subpopulations: Insights from a novel human angiogenesis assay. *J Am Coll Cardiol* 2008;51:660–668.
- 13 Somani A, Nguyen J, Milbauer LC et al. The establishment of murine blood outgrowth endothelial cells and observations relevant to gene therapy. *Transl Res* 2007;150:30–39.
- 14 Lin Y, Weisdorf DJ, Solovey A et al. Origins of circulating endothelial cells and endothelial outgrowth from blood. *J Clin Invest* 2000;105:71–77.
- 15 Matsui H, Shibata M, Brown B et al. Ex vivo gene therapy for hemophilia A that enhances safe delivery and sustained in vivo factor VIII expression from lentivirally engineered endothelial progenitors. *Stem Cells* 2007;25:2660–2669.
- 16 Vermeulen P, Dickens S, Degezelle K et al. A plasma-based biomatrix mixed with endothelial progenitor cells and keratinocytes promotes matrix formation, angiogenesis, and reepithelialization in full-thickness wounds. *Tissue Eng Part A* 2008;15:1533–1542.
- 17 Aranguren XL, Verfaillie CM, Luttun A. Emerging hurdles in stem cell therapy for peripheral vascular disease. *J Mol Med* 2009;87:3–16.
- 18 Smadja DM, Bieche I, Silvestre JS et al. Bone morphogenetic proteins 2 and 4 are selectively expressed by late outgrowth endothelial progenitor cells and promote neoangiogenesis. *Arterioscler Thromb Vasc Biol* 2008;28:2137–2143.
- 19 Kung EF, Wang F, Schechner JS. In vivo perfusion of human skin substitutes with microvessels formed by adult circulating endothelial progenitor cells. *Dermatol Surg* 2008;34:137–146.
- 20 Fuchs S, Ghanaati S, Orth C et al. Contribution of outgrowth endothelial cells from human peripheral blood on in vivo vascularization of bone tissue engineered constructs based on starch polycaprolactone scaffolds. *Biomaterials* 2009;30:526–534.
- 21 Dudek AZ, Bodempudi V, Welsh BW et al. Systemic inhibition of tumour angiogenesis by endothelial cell-based gene therapy. *Br J Cancer* 2007;97:513–522.
- 22 Liu Y, Dulchavsky DS, Gao X et al. Wound repair by bone marrow stromal cells through growth factor production. *J Surg Res* 2006;136:336–341.
- 23 Cha J, Falanga V. Stem cells in cutaneous wound healing. *Clin Dermatol* 2007;25:73–78.
- 24 Bennett SP, Griffiths GD, Schor AM et al. Growth factors in the treatment of diabetic foot ulcers. *Br J Surg* 2003;90:133–146.
- 25 Cianfarani F, Zambruno G, Brogelli L et al. Placenta growth factor in diabetic wound healing: Altered expression and therapeutic potential. *Am J Pathol* 2006;169:1167–1182.
- 26 Dickens S, Vermeulen P, Hendrickx B et al. Regulable vascular endothelial growth factor165 overexpression by ex vivo expanded keratinocyte cultures promotes matrix formation, angiogenesis, and healing in porcine full-thickness wounds. *Tissue Eng Part A* 2008;14:19–27.
- 27 MacNeil S. Progress and opportunities for tissue-engineered skin. *Nature* 2007;445:874–880.
- 28 Hill JM, Zalos G, Halcox JP et al. Circulating endothelial progenitor cells, vascular function, and cardiovascular risk. *N Engl J Med* 2003;348:593–600.
- 29 Gallez B, Baudelet C, Jordan BF. Assessment of tumor oxygenation by electron paramagnetic resonance: Principles and applications. *NMR Biomed* 2004;17:240–262.
- 30 Luttun A, Lupu F, Storkebaum E et al. Lack of plasminogen activator inhibitor-1 promotes growth and abnormal matrix remodeling of advanced atherosclerotic plaques in apolipoprotein E-deficient mice. *Arterioscler Thromb Vasc Biol* 2002;22:499–505.
- 31 Hirschberg R, Wang S, Mitu GM. Functional symbiosis between endothelium and epithelial cells in glomeruli. *Cell Tissue Res* 2008;331:485–493.
- 32 Chavakis E, Aicher A, Heeschen C et al. Role of beta2-integrins for homing and neovascularization capacity of endothelial progenitor cells. *J Exp Med* 2005;201:63–72.
- 33 Kiran MS, Sameer Kumar VB, Viji RI et al. Temporal relationship between MMP production and angiogenic process in HUVECs. *Cell Biol Int* 2006;30:704–713.
- 34 Swope VB, Boyce ST. Differential expression of matrix metalloproteinase-1 in vitro corresponds to tissue morphogenesis and quality assurance of cultured skin substitutes. *J Surg Res* 2005;128:79–86.
- 35 Luttun A, Tjwa M, Moons L et al. Revascularization of ischemic tissues by PIGF treatment, and inhibition of tumor angiogenesis, arthritis and atherosclerosis by anti-Flt1. *Nat Med* 2002;8:831–840.
- 36 Gaengel K, Genove G, Armulik A et al. Endothelial-mural cell signaling in vascular development and angiogenesis. *Arterioscler Thromb Vasc Biol* 2009;29:630–638.
- 37 Kandyba EE, Hodgins MB, Martin PE. A murine living skin equivalent amenable to live-cell imaging: Analysis of the roles of connexins in the epidermis. *J Invest Dermatol* 2008;128:1039–1049.
- 38 Harrison CA, MacNeil S. The mechanism of skin graft contraction: An update on current research and potential future therapies. *Burns* 2008;34:153–163.
- 39 Badillo AT, Redden RA, Zhang L et al. Treatment of diabetic wounds with fetal murine mesenchymal stromal cells enhances wound closure. *Cell Tissue Res* 2007;329:301–311.
- 40 Chen L, Tredget EE, Wu PY et al. Paracrine factors of mesenchymal stem cells recruit macrophages and endothelial lineage cells and enhance wound healing. *Plos One* 2008;3:e1886.
- 41 Wu Y, Chen L, Scott PG et al. Mesenchymal stem cells enhance wound healing through differentiation and angiogenesis. *Stem Cells* 2007;25:2648–2659.
- 42 Au P, Daheron LM, Duda DG et al. Differential in vivo potential of endothelial progenitor cells from human umbilical cord blood and adult peripheral blood to form functional long-lasting vessels. *Blood* 2008;111:1302–1305.
- 43 van Beem RT, Verloop RE, Kleijer M et al. Blood outgrowth endothelial cells from cord blood and peripheral blood: Angiogenesis-related characteristics in vitro. *J Thromb Haemost* 2009;7:217–226.
- 44 Corselli M, Parodi A, Moggi M et al. Clinical scale ex vivo expansion of cord blood-derived outgrowth endothelial progenitor cells is associated with high incidence of karyotype aberrations. *Exp Hematol* 2008;36:340–349.
- 45 Bluff JE, Ferguson MW, O’Kane S et al. Bone marrow-derived endothelial progenitor cells do not contribute significantly to new vessels during incisional wound healing. *Exp Hematol* 2007;35:500–506.
- 46 Dengler TJ, Pober JS. Human vascular endothelial cells stimulate memory but not naive CD8+ T cells to differentiate into CTL retaining an early activation phenotype. *J Immunol* 2000;164:5146–5155.
- 47 Lamme EN, van Leeuwen RT, Mekkes JR et al. Allogeneic fibroblasts in dermal substitutes induce inflammation and scar formation. *Wound Repair Regen* 2002;10:152–160.
- 48 O’Toole EA, Marinkovich MP, Peavey CL et al. Hypoxia increases human keratinocyte motility on connective tissue. *J Clin Invest* 1997;100:2881–2891.
- 49 Kan C, Abe M, Yamanaka M et al. Hypoxia-induced increase of matrix metalloproteinase-1 synthesis is not restored by reoxygenation in a three-dimensional culture of human dermal fibroblasts. *J Dermatol Sci* 2003;32:75–82.
- 50 Pierce GF, Vande Berg J, Rudolph R et al. Platelet-derived growth factor-BB and transforming growth factor beta 1 selectively modulate glycosaminoglycans, collagen, and myofibroblasts in excisional wounds. *Am J Pathol* 1991;138:629–646.
- 51 Lee JA, Conejero JA, Mason JM et al. Lentiviral transfection with the PDGF-B gene improves diabetic wound healing. *Plast Reconstr Surg* 2005;116:532–538.
- 52 Kyriakides TR, Wulsin D, Skokos EA et al. Mice that lack matrix metalloproteinase-9 display delayed wound healing associated with delayed reepithelialization and disordered collagen fibrillogenesis. *Matrix Biol* 2009;28:65–73.



See www.StemCells.com for supporting information available online.